

# In-medium properties of light vector and axial-vector mesons: effects of magnetic catalysis

Pallabi Parui\* and Amruta Mishra†

*Department of Physics, Indian Institute of Technology, Delhi, New Delhi - 110016*

## Abstract

The in-medium masses of the light vector,  $\rho^{0,\pm}$ ,  $\omega$  and axial-vector meson,  $A_1^{0,\pm}$ , are studied in the magnetized nuclear matter, accounting for the effects of magnetic catalysis. The in-medium partial decay widths for the  $A_1 \rightarrow \rho\pi$  channels, are studied from the in-medium masses of the initial and the final state particles, by applying a phenomenological Lagrangian to account for the  $A_1\rho\pi$  interaction vertices. The masses calculated within the QCD sum rule framework, are obtained in terms of the light quark ( $\sim \langle \bar{q}q \rangle$ ) and the scalar gluon condensates ( $\sim \langle G^2 \rangle$ ), as well as the light four-quark condensate ( $\sim \langle \bar{q}q \rangle^2$ ). The condensates are calculated within the chiral  $SU(3)$  model in terms of the medium modified scalar fields, which in turn are proportional to the chiral condensates. The effects of magnetic field are incorporated through the Fermi and Dirac sea of nucleons within the chiral effective model. The scalar fields and hence the chiral condensates tend to rise with magnetic field due to the magnetized Dirac sea contribution, an effect called magnetic catalysis. The effects of magnetic field on the in-medium hadronic decay widths are seen to be appreciable through the catalysis effect, which may affect the light mesons production in the non-central, heavy-ion collision experiments, where estimated magnetic field is very large.

---

\*Electronic address: pallabiparui123@gmail.com

†Electronic address: amruta@physics.iitd.ac.in

## I. INTRODUCTION

The study of the in-medium hadronic properties (masses, decay widths etc.), under extreme conditions of density and/or temperature, has become a very important topic of research in the strong interaction physics. The study is of great relevance in the ultra relativistic, heavy-ion collision experiments and in the investigation of the size, equation of states of some astrophysical objects, for e.g., neutron stars. In the peripheral, ultra relativistic, heavy-ion collision experiments, huge magnetic fields have been estimated, of the order of  $eB \approx 2m_\pi^2$  at RHIC in BNL and  $eB \approx 15m_\pi^2$  at LHC in CERN [1]-[5]. Thus, the in-medium study of hadrons, in the presence of an external, strong magnetic field background, attracts a lot of research interest in this area. The large number difference between the neutrons and protons of the heavy colliding nuclei, leads to the incorporation of the effects of isospin asymmetry on the study of hadronic properties.

The light axial-vector meson,  $A_1$  with isospin  $I = 1$  and the quantum numbers,  $J^{PC} = 1^{++}$ , is considered to be the chiral partner of the much lighter vector meson,  $\rho$  with  $I^G(J^{PC}) = 1^+(1^{--})$ . The medium modifications of the properties of the light vector mesons can affect the low mass dilepton production [6] in the heavy-ion collision experiments. The heavy leptonic decay of  $\tau \rightarrow \nu_\tau + X$ , makes it possible to determine the coupling of a hadronic state,  $X$  to the axial-vector current. Its decay fraction to the three pion states through the intermediate state of  $\rho\pi$  with respect to the total width, shows that the dominant decay mode of the  $A_1$  meson is the partial ( $s$ -wave)  $\rho\pi$  mode [7]. The study of the in-medium spectral properties of the  $A_1$  meson is important in the context of partial restoration of chiral symmetry and to provide valuable information to further experimental studies of the axial-vector meson state. There are some well known properties of the axial-vector state, for e.g., its current coupling to the  $\pi$  meson,  $f_\pi$ , which is defined in the usual way of  $\langle 0 | \bar{u} \gamma_\mu \gamma_5 d | \pi \rangle = i f_\pi P_\mu$  [8]. The fundamental symmetry of Quantum chromodynamics (QCD) is the chiral symmetry, which is spontaneously broken at low densities and low temperatures due to the non-zero expectation values of the QCD vacuum condensates. The formation of the quark and gluon condensates in QCD vacuum, leads to the generation of hadron masses. The spontaneous chiral symmetry breaking effect induces mass splittings between the chiral partners in the spectra of light hadrons, for e.g.,  $\pi$ - $\sigma$ ,  $\rho$ - $A_1$ . The condensates are expected to change with temperature and/or density, and also with the magnetic field. The values tend to decrease

with increasing density and temperature [9–11], but there is an enhancement of the chiral condensates with increasing magnetic fields, a phenomenon called magnetic catalysis [12–14]. In the literature, there are very few studies on the magnetic catalysis effects of hadronic properties in the nuclear matter environment. There have been some quark matter studies, in the context of the Nambu Jona Lasinio model [15–19]. The effects of magnetic catalysis have been studied on the nuclear matter phase transition in the framework of Walecka model and an extended linear sigma model [20], resulting in the increasing mass of the nucleon as a function of the magnetic field, at zero baryon density and zero moments of the nucleons. The effect of catalysis effect was observed indirectly through the scalar field dependency of the nucleon mass ( $M_N = m_N - g_\sigma \sigma$ ), where the scalar fields are related to the chiral condensates. In [21], the effects of magnetized Dirac sea have been studied under the weak-field approximation of a constant, external magnetic field. An increase of the nucleon mass with magnetic field was observed within the Walecka model, at zero density, in addition to some significant contribution from the anomalous magnetic moments of the Dirac sea of nucleons. At finite temperature, an inverse magnetic catalysis effect [22] was observed on the critical temperature of nuclear matter phase transition, i.e., lowering of the condensates with magnetic field. At higher temperatures and densities, the chiral symmetric phase is expected to be (partially) restored, which can be inferred from its observable consequence on the hadron spectrum. The dilepton data, as measured in the relativistic heavy-ion collisions, provided evidence on the in-medium spectral changes of  $\rho$  meson, while there is very little access to the experimental evidence on the in-medium  $A_1$  spectral properties. Therefore, to investigate on the chiral symmetry restoration from the in-medium spectral changes of the  $\rho$  meson [23], a theoretical investigations of the same is required on the  $A_1$  meson spectrum. Towards this aim, sum rules serve as a good non-perturbative tool to connect the hadronic spectral properties directly to the QCD vacuum condensates. The medium modifications of the spectral properties (for e.g., mass, decay width) of hadrons thus observed, may be used as good signals to the changes in the QCD vacuum condensates.

There have been QCD sum rule studies for the spectral density induced by the axial-vector current [8, 24]. In these works, Borel sum rules have been constructed for the axial-vector current and its divergence, which lead to the same mass value for  $A_1^0$  at a particular value of the continuum threshold,  $s_0$  [25]. The spectral functions of the  $\rho$  and  $A_1$  mesons have been analyzed in vacuum using the hadronic models (constrained by the experimental data

and the Weinberg-type sum rule) and have been tested further with QCD sum rules [26]. The Weinberg-type sum rules [27] for the  $\rho$  and  $A_1$  mesons (in the exact chiral limit), have been studied at zero and finite temperature in ref.[28]; thorough discussion were given on the possible relations between the chiral symmetry restoration and the various types of finite temperature sum rules. In ref. [29], finite temperature ( $T \neq 0$ ) study of  $\rho$ ,  $\omega$  and  $A_1$  mesons, by using the Borel transformed sum rule, have been performed. The study has shown a dropping  $A_1$  mass with  $T$ . The temperature effect have been incorporated through the thermal average of the local operators in the operator product expansion, which leads to the non-vanishing values of Lorentz non-scalar operators that would have otherwise been zero at  $T=0$ . The in-medium changes of the scalar four-quark condensates have been found to play significant role on these meson properties. In ref.[30], the Breit-Wigner parametrization for the  $\rho$ ,  $A_1$  spectral functions have been used and the constraints of QCD sum rules have been investigated on their masses and decay widths, in vacuum and at finite nuclear density. The effect of the pion coupling to the axial current have been considered by adding a  $\delta$ -function peak at  $m_\pi$ , to the correlator of axial-vector channel. In ref.[31], the parity-mixing ansatz including the finite widths of  $\rho$ ,  $A_1$  spectra have been investigated at finite temperature in the context of finite energy sum rules. A decreasing  $A_1$  meson mass with temperature has been observed, which might indicate the expected tendency of  $\rho$  - $A_1$  mass degeneracy in the nearby critical temperature,  $T_c$  for chiral symmetry restoration. In ref.[32], the effects of magnetic field have been studied on the in-medium masses of the light vector mesons ( $\rho$ ,  $\omega$ ,  $\phi$ ), in the nuclear matter environment, by using the sum rule method. In-medium masses are obtained by incorporating the medium effects through the scalar fields, calculated within the chiral  $SU(3)$  model. In the absence of an external magnetic field, masses have been studied in the strange hadronic matter, using the sum rule approach [9], in terms of the condensates calculated within the chiral model via the scalar fields. In ref.[32], magnetic field contributed through the Landau quantization of protons and the anomalous magnetic moments of both the nucleons in the Fermi sea. In our present study, effects from the magnetized Dirac sea are incorporated additionally, to study the effects of magnetic catalysis on the in-medium masses and decay widths of  $\rho$ ,  $\omega$  and  $A_1$  mesons at finite magnetic field. The present paper is organized as follows. In Sec.II, the chiral effective model is discussed to find the in-medium quark and gluon condensates. In Sec.III, QCD sum rule approach is presented to calculate the masses of the light vector and axial-vector mesons. Sec.IV,

describes the phenomenological Lagrangian formulation to find the hadronic decays of the  $A_1$  meson. The results of the present investigation are discussed in Sec.V Finally, Sec.VI, summarizes the findings of the present work.

## II. THE CHIRAL EFFECTIVE LAGRANGIAN

In the present investigation, the in-medium masses of the light vector and axial-vector mesons are calculated within the sum rule approach, by determining the QCD condensates in a chiral effective model. The effective chiral model is based on the non-linear realization of chiral  $SU(3)_L \times SU(3)_R$  symmetry [33–35] and the broken scale-invariance of QCD [36–38]. A scale-invariance breaking logarithmic potential in the scalar dilaton field,  $\chi$  is introduced [39, 40], which simulates the gluon condensate of QCD. The Lagrangian density of the chiral  $SU(3)$  model can be generalized as [38],

$$\mathcal{L} = \mathcal{L}_{kin} + \mathcal{L}_{BM} + \mathcal{L}_{vec} + \mathcal{L}_0 + \mathcal{L}_{scale-break} + \mathcal{L}_{SB} + \mathcal{L}_{mag} \quad (1)$$

$\mathcal{L}_{kin}$  is the kinetic energy of the baryons and the mesons degrees of freedom;  $\mathcal{L}_{BM}$  represents the baryon-mesons (both spin-0 and spin-1 mesons) interactions;  $\mathcal{L}_{vec}$  contains the quartic self-interactions of the vector mesons and their couplings with the scalar ones;  $\mathcal{L}_0$  incorporates the spontaneous chiral symmetry breaking effects via meson-meson interactions;  $\mathcal{L}_{scale-break}$  is the scale symmetry breaking logarithmic potential; and  $\mathcal{L}_{SB}$  is the explicit symmetry breaking term; finally the effects of the magnetic field on the charged and neutral baryons in the nuclear medium are incorporated through [41–47]

$$\mathcal{L}_{mag} = -\frac{1}{4}F_{\mu\nu}F^{\mu\nu} - e_i\bar{\psi}_i\gamma_\mu A^\mu\psi_i - \frac{1}{4}\kappa_i\mu_N\bar{\psi}_i\sigma^{\mu\nu}F_{\mu\nu}\psi_i \quad (2)$$

where,  $\psi_i$  is the baryon field operator for  $i^{th}$  ( $i = p, n$ ) baryon with electric charge  $e_i$ , in the nuclear matter. The parameters,  $\kappa_p(i = p) = 3.5856$  and  $\kappa_n(i = n) = -3.8263$ , are the gyromagnetic ratio corresponding to the anomalous magnetic moments (AMM) of the proton and the neutron, respectively [46, 47]. In the magnetized nuclear medium, the magnetic field contributions are coming through the Landau energy levels of the protons and the anomalous magnetic moments of the nucleons in the Fermi sea. The Dirac sea effects at finite magnetic field, are incorporated through an additional term in the scalar densities of the nucleons which correspond to the one-loop, self-energy functions of Dirac sea of nucleons, calculated

by their medium modified fermionic propagator [21, 48].

The concept of broken scale-invariance of QCD is incorporated in the chiral model at the tree level, through a logarithmic potential in the scalar dilaton field  $\chi$  [39, 40], as

$$\mathcal{L}_{scale-break} = -\frac{1}{4}\chi^4 \ln\left(\frac{\chi^4}{\chi_0^4}\right) + \frac{d}{3}\chi^4 \ln\left(\left(\frac{(\sigma^2 - \delta^2)\zeta}{\sigma_0^2\zeta_0}\right)\left(\frac{\chi}{\chi_0}\right)^3\right) \quad (3)$$

where,  $\sigma$ ,  $\zeta$  are the non-strange, strange scalar isoscalar fields, respectively and  $\delta$  is the scalar isovector field; The Lagrangian parameter,  $d$  is chosen to be 0.064 [38, 49]. The subscript-0 in the fields indicate their respective vacuum expectation values. The scale-invariance breaking phenomena of QCD leads to the trace anomaly of QCD, i.e., non-zero value for the trace of the energy-momentum tensor in QCD, which in the limit of finite light quark masses  $m_i (i = u, d, s)$  become [32, 50]

$$T_\mu^\mu = \sum_{i=u,d,s} m_i \langle \bar{q}_i q_i \rangle + \left\langle \frac{\beta_{QCD}}{2g} G_{\mu\nu}^a G^{a\mu\nu} \right\rangle \quad (4)$$

In Eq.(4),  $G_{\mu\nu}^a$  is the gluon field strength tensor of QCD which is simulated in the chiral effective Lagrangian at the tree level through Eq.(3). The trace of the energy momentum tensor within the model can be obtained from the Lagrangian density containing the field  $\chi$  [9, 51, 52]

$$\theta_\mu^\mu = \chi \frac{\partial \mathcal{L}}{\partial \chi} - 4\mathcal{L} = -(1-d)\chi^4 \quad (5)$$

The first term in Eq.(4) corresponds to the explicit chiral symmetry breaking term in QCD

$$\mathcal{L}_{SB}^{QCD} = -Tr[diag(m_u \bar{u}u, m_d \bar{d}d, m_s \bar{s}s)] \quad (6)$$

which in the chiral  $SU(3)$  model under the mean-field approximation is written as [9]

$$\mathcal{L}_{SB} = Tr \left[ diag \left( -\frac{1}{2}m_\pi^2 f_\pi (\sigma + \delta), -\frac{1}{2}m_\pi^2 f_\pi (\sigma - \delta), \left( \sqrt{2}m_k^2 f_k - \frac{1}{\sqrt{2}}m_\pi^2 f_\pi \right) \zeta \right) \right] \quad (7)$$

Comparing Eqs. (6) and (7), the light quark condensates can be related to the scalar fields  $\sigma$ ,  $\zeta$  and  $\delta$  as

$$m_u \langle \bar{u}u \rangle = \frac{1}{2}m_\pi^2 f_\pi (\sigma + \delta) \quad (8)$$

$$m_d \langle \bar{d}d \rangle = \frac{1}{2}m_\pi^2 f_\pi (\sigma - \delta) \quad (9)$$

$$m_s \langle \bar{s}s \rangle = \left( \sqrt{2}m_k^2 f_k - \frac{1}{\sqrt{2}}m_\pi^2 f_\pi \right) \zeta \quad (10)$$

From Eqs. (4) and (5), one obtains the scalar gluon condensate as

$$\theta_\mu^\mu = \sum_{i=u,d,s} m_i \bar{q}_i q_i - \frac{9}{8} \left\langle \frac{\alpha_s}{\pi} G_{\mu\nu}^a G^{a\mu\nu} \right\rangle = -(1-d)\chi^4 \quad (11)$$

In the above,  $\beta_{QCD}(g) = -\frac{N_c g^3}{48\pi^2} (11 - \frac{2}{N_c} N_f) = -\frac{9\alpha_s}{8\pi} 2g$ , the QCD  $\beta$  function at one-loop level has been used with  $N_f = 3$  flavors,  $N_c = 3$  colors of quarks and  $\alpha_s = \frac{g^2}{4\pi}$ ; by using the expressions for  $m_i \langle \bar{q}_i q_i \rangle$ , ( $i = u, d, s$ ) from Eqs. (8)-(10) the final expression for the gluon condensate is given by

$$\left\langle \frac{\alpha_s}{\pi} G_{\mu\nu}^a G^{a\mu\nu} \right\rangle = \frac{8}{9} \left[ (1-d)\chi^4 + \left( m_\pi^2 f_\pi \sigma + \left( \sqrt{2} m_k^2 f_k - \frac{1}{\sqrt{2}} m_\pi^2 f_\pi \right) \zeta \right) \right] \quad (12)$$

The coupled equations of motion for the scalar fields  $\sigma$ ,  $\zeta$ ,  $\delta$  and  $\chi$ , as derived from the chiral  $SU(3)$  Lagrangian under the mean-field approximation, are solved in strongly magnetized, isospin asymmetric nuclear matter. In these coupled equations of motion [51], the number and scalar densities of nucleons ( $\rho_i, \rho_i^s; i = p, n$ ) incorporate the effects of the Landau energy levels of protons and the anomalous magnetic moments of nucleons from the magnetized Fermi sea of nucleons [46, 47]. The scalar densities of the protons and neutrons incorporate additional contribution from the magnetized Dirac sea, by deriving the fermionic tadpole diagrams in presence of a background magnetic field, accounting for the nucleons anomalous magnetic moments [21]. The enhanced values of the scalar fields with increasing magnetic field represent the magnetic catalysis effect indirectly, as the fields are proportional to the chiral condensate as given by Eqs.(8)-(10), and Eq.(12). Thus, the effects of magnetic catalysis in terms of the scalar fields from the chiral model, are studied on the in-medium masses of  $\rho$ ,  $\omega$  and  $A_1$  mesons, in the next section, by using the sum rule approach.

### III. QCD SUM RULE FRAMEWORK

The masses of the charged and charge neutral light axial-vector meson,  $A_1^\pm$ ,  $A_1^0$ , light vector meson,  $\rho^\pm$ ,  $\rho_0$  and  $\omega$  are calculated using the QCD sum rule approach. The in-medium masses are obtained in terms of the light quark condensates (including the scalar four-quark condensate) and the scalar gluon condensate, calculated from the chiral  $SU(3)$  model. The time-ordered current-current correlator is given by [8, 24]

$$\Pi_{\mu\nu}(q) = i \int d^4x e^{iqx} \langle T[J_\mu(x), J_\nu(0)] \rangle. \quad (13)$$

where  $T$  denotes the time-ordered product, and the symbol  $\langle \rangle$  indicates the in-medium expectation value of the  $T$ -ordered product of currents. The quark-bilinears of currents for all three axial-vector states (with  $J^P = 1^+$ ) are defined as

$$J_\mu^{(A_1^+)} = \bar{d}\gamma_\mu\gamma_5 u; \quad J_\mu^{(A_1^-)} = \bar{u}\gamma_\mu\gamma_5 d; \quad J_\mu^{(A_1^0)} = \frac{1}{2}(\bar{u}\gamma_\mu\gamma_5 u - \bar{d}\gamma_\mu\gamma_5 d) \quad (14)$$

For the vector currents (with  $J^P = 1^-$ )

$$J_\mu^{(\rho^+)} = \bar{d}\gamma_\mu u; \quad J_\mu^{(\rho^-)} = \bar{u}\gamma_\mu d; \quad J_\mu^{(\omega, \rho^0)} = \frac{1}{2}(\bar{u}\gamma_\mu u \pm \bar{d}\gamma_\mu d) \quad (15)$$

The correlation function can be written into the following tensor structure [24, 30, 53, 54]

$$\Pi_{\mu\nu}(q) = q_\mu q_\nu R(q^2) - g_{\mu\nu} K(q^2) \quad (16)$$

This expression is valid for mesons at rest. For the conserved vector currents,  $K(q^2) = q^2 R(q^2)$ . As for the non-conserved, axial-vector current, this relation no longer holds, and  $R(q^2)$  has contributions from pseudoscalar mesons [8, 24, 53, 54]. In principle, sum rule can be carried out with either  $R(q^2)$  or  $K(q^2)$  [24]. Further studies in this work are based on  $R(q^2)$ , following the arguments given in ref.[30], for the axial-vector current.

There are two representations of the current-current correlator. On the phenomenological side,  $R(q^2)$  is related to its imaginary part via the dispersion relation [9, 54]

$$R_{phen.}(q^2) = \frac{1}{\pi} \int_0^\infty ds \frac{Im R^{phen.}(s)}{(s - q^2)} \quad (17)$$

Here  $Im R^{phen.}(s)$ , also called the spectral density, is parametrized by the hadronic resonance and the perturbative continuum part. The other representation is to express the real part of the correlation function by the Wilson's operator product expansion (OPE), which in the large space like region ( $Q^2 = -q^2 >> 1 \text{ GeV}^2$ ) [29, 30, 55], is given by

$$R_{OPE}(q^2 = -Q^2) = \left( -c_0 \ln \left( \frac{Q^2}{\mu^2} \right) + \frac{c_1}{Q^2} + \frac{c_2}{Q^4} + \frac{c_3}{Q^6} + \dots \right) \quad (18)$$

In the present study, the operators up to dimension-6 are considered and the scale  $\mu$  has been chosen as 1 GeV [9, 29, 55]. The first term in the OPE is a contribution from perturbative QCD. The coefficients  $c_i$  ( $i = 1, 2, 3$ ) of the subsequent terms, contained the QCD non-perturbative effects in terms of the quark and gluon degrees of freedom and some parameters from the QCD Lagrangian. The condensates are affected in presence of a medium. The coefficient,  $c_3$  is being associated with the light four-quark condensate and it is different



corresponding to the different current quark-bilinears of the charged and neutral mesons with the same  $J^{PC}$  quantum numbers. In Eq.(18), the  $c_i$  ( $i = 0, 1, 2, 3$ ) coefficients for the light axial-vector meson,  $A_1$  are given by [29, 30, 54, 56]

$$c_0 = \frac{1}{8\pi^2} \left(1 + \frac{\alpha_s}{\pi}\right) \quad (19)$$

$$c_1 = -\frac{3}{8\pi^2} (m_u^2 + m_d^2) \quad (20)$$

$$c_2 = \frac{1}{24} \left\langle \frac{\alpha_s}{\pi} G^{\mu\nu} G_{\mu\nu} \right\rangle - \frac{1}{2} \langle m_u \bar{u}u + m_d \bar{d}d \rangle \quad (21)$$

$$c_3^{(A_1^0)} = -\frac{\pi}{2} \alpha_s \left[ \left\langle (\bar{u}\gamma_\mu \lambda^a u - \bar{d}\gamma_\mu \lambda^a d)^2 \right\rangle + \frac{2}{9} \left\langle (\bar{u}\gamma_\mu \lambda^a u + \bar{d}\gamma_\mu \lambda^a d) \times \left( \sum_{q=u,d,s} \bar{q}\gamma^\mu \lambda^a q \right) \right\rangle \right] = \pi \alpha_s \times \frac{88}{81} \kappa_1 (\langle \bar{u}u \rangle^2 + \langle \bar{d}d \rangle^2) \quad (22)$$

$$c_3^{(A_1^\pm)} = -\frac{\pi}{2} \alpha_s \left[ 2 \left\langle (\bar{u}\gamma_\mu \lambda^a d) (\bar{d}\gamma_\mu \lambda^a u) \right\rangle + \frac{2}{9} \left\langle (\bar{u}\gamma_\mu \lambda^a u + \bar{d}\gamma_\mu \lambda^a d) \times \left( \sum_{q=u,d,s} \bar{q}\gamma^\mu \lambda^a q \right) \right\rangle \right] = \pi \alpha_s \times \kappa_2 \left[ \frac{16}{81} (\langle \bar{u}u \rangle^2 + \langle \bar{d}d \rangle^2) + \frac{16}{9} \langle \bar{u}u \rangle \langle \bar{d}d \rangle \right] \quad (23)$$

The first three coefficients,  $c_i$  ( $i = 0, 1, 2$ ) are same for the charged and neutral  $A_1$  mesons. To simplify the expression for the scalar four-quark condensates, the use of the factorization method [24, 25] is adopted

$$-\langle (\bar{q}_i \gamma_\mu \lambda^a q_j)^2 \rangle = \langle (\bar{q}_i \gamma_\mu \gamma_5 \lambda^a q_j)^2 \rangle = \delta_{ij} \frac{16}{9} \kappa_j \langle \bar{q}_i q_j \rangle^2 \quad (24)$$

The parameter  $\kappa_j$  here, introduces deviation from the exact factorization [9] (which is  $\kappa_j = 1$  in the vacuum saturation assumption [24, 57]). The value of the running coupling constant is  $\alpha_s = 0.35$ , at  $\mu = 1$  GeV scale, as in refs.[9, 29]. For the (neutral) vector meson channels of  $\rho$  and  $\omega$ , the Wilson coefficients are taken from refs.[9, 32] in order to calculate the effects of magnetic catalysis on their masses. For the charged  $\rho$  meson channel, the first three coefficients ( $c_i; i = 0, 1, 2$ ) in the OPE are same as its neutral partner ( $\rho_0$ ). The  $c_3$  term is different in the following way

$$c_3^{\rho^\pm} = -\frac{\pi}{2} \alpha_s \left[ 2 \left\langle (\bar{u}\gamma_\mu \gamma^5 \lambda^a d) (\bar{d}\gamma_\mu \gamma^5 \lambda^a u) \right\rangle + \frac{2}{9} \left\langle (\bar{u}\gamma_\mu \lambda^a u + \bar{d}\gamma_\mu \lambda^a d) \times \left( \sum_{q=u,d,s} \bar{q}\gamma^\mu \lambda^a q \right) \right\rangle \right] = \pi \alpha_s \times \kappa_3 \left[ \frac{16}{81} (\langle \bar{u}u \rangle^2 + \langle \bar{d}d \rangle^2) - \frac{16}{9} \langle \bar{u}u \rangle \langle \bar{d}d \rangle \right] \quad (25)$$

The QCD sum rule, thus connects the hadronic spectral properties in terms of the resonance parameters given by Eq.(17), to the non-perturbative effects of QCD through the quark and gluon condensates in Eq.(18), with  $c_i$ 's given by Eqs.(19)-(25).

In practice, the parametrization of the current-current correlator is given for the energy region of the lowest hadronic resonance, usually there is no model which can be valid for arbitrary high energies. In this purpose, it is desirable to achieve a larger suppression on the high energy part of the hadronic spectral distribution, which is least accessible. Borel transform is applied in this aim. It is defined on an arbitrary function  $g$  as [54]

$$g(Q^2) \xrightarrow{\hat{B}} \tilde{g}(M^2) \quad (26)$$

$$\hat{B} := \lim_{Q^2 \rightarrow \infty, n \rightarrow \infty} \frac{1}{\Gamma(n)} (-Q^2)^n \left( \frac{d}{dQ^2} \right)^n. \quad (27)$$

with  $Q^2/n = M^2$  become fixed and  $M$  is called the Borel mass. By the application of Borel transform, the phenomenological side of Eq.(17) is connected to the OPE side in Eq.(18) as

$$\frac{1}{\pi} \int_0^\infty ds e^{-s/M^2} \text{Im} R^{\text{phen.}}(s) = \left[ c_0 M^2 + c_1 + \frac{c_2}{M^2} + \frac{c_3}{2M^4} \right] \quad (28)$$

The exponential function on the l.h.s enhances the effect of the ground state by suppressing the continuum part at large  $s$ . The higher dimensional operators of the  $R_{OPE}$ , on the r.h.s, are suppressed by an additional factor of  $1/(n-1)!$ ; which leads to the better convergence of the operator product expansion.

The hadronic spectral density function,  $\text{Im} R^{\text{phen.}}(s)$  separates into a resonance part,  $R_{res}(s)$  (for  $s \leq s_0$ ) and a perturbative continuum (for large  $s$ ) [9, 30, 55]

$$\frac{\text{Im} R^{\text{phen.}}(s)}{\pi} = R_{res}(s) \Theta(s_0 - s) + c_0 \Theta(s - s_0) \quad (29)$$

Where  $s_0$  is the threshold between the low energy resonance region and the high energy continuum part, latter being calculated in perturbative QCD.

Next, the finite energy sum rules (FESRs) are derived by inserting Eq.(29) into the l.h.s of Eq.(28). The exponential function then expanded in powers of  $\frac{s}{M^2}$  for  $s \leq s_0$ , and  $M > \sqrt{s_0}$ . Equating the various powers of  $1/M^2$  on both sides of Eq.(28), after this expansion, the finite energy sum rules in vacuum, can be written as

$$\int_0^{s_0} ds R_{res}(s) = (c_0 s_0 + c_1) \quad (30)$$

$$\int_0^{s_0} ds s R_{res}(s) = \left( \frac{c_0 s_0^2}{2} - c_2 \right) \quad (31)$$

$$\int_0^{s_0} ds s^2 R_{res}(s) = \left( \frac{c_0 s_0^3}{3} + c_3 \right) \quad (32)$$

The parametrization of the spectral function,  $R_A^{phen.}(s)$  used in the present study for the axial-vector channel is

$$R_A^{phen.}(s) = F_A \delta(s - m_A^2) + c_0 \Theta(s - s_0^A) + f_\pi^2 \delta(s - m_\pi^2) \quad (33)$$

Where,  $\frac{Im R^{phen.}(s)}{\pi} = R^{phen.}(s)$ . In the axial-vector channel, apart from the  $A_1$  resonance term, there is a contribution from the pseudoscalar meson resonance, as it has been considered in [8, 24, 30]. The simple ansatz for the vector meson channel is given by [9, 29, 32, 55]

$$R_V^{phen.}(s) = F_V \delta(s - m_V^2) + c_0 \Theta(s - s_0^V) \quad (34)$$

Inserting the expression (33) into Eqs.(30)-(32), the finite energy sum rules for the axial-vector channel, in the vacuum, are given by

$$F_A = (c_0 s_0^A + c_1 - f_\pi^2) \quad (35)$$

$$F_A m_A^2 = \left( \frac{c_0 (s_0^A)^2}{2} - c_2 - f_\pi^2 m_\pi^2 \right) \quad (36)$$

$$F_A m_A^4 = \left( \frac{c_0 (s_0^A)^3}{3} + c_3^A - f_\pi^2 m_\pi^4 \right) \quad (37)$$

In the same way, for the vector meson channel in the vacuum, using Eq.(34) into Eqs.(30)-(32), one obtains

$$F_V = (c_0 s_0^V + c_1) \quad (38)$$

$$F_V m_V^2 = \left( \frac{c_0 (s_0^V)^2}{2} - c_2 \right) \quad (39)$$

$$F_V m_V^4 = \left( \frac{c_0 (s_0^V)^3}{3} + c_3^V \right) \quad (40)$$

In the nuclear medium, for mesons at rest, the meson-nucleon scattering effect is incorporated through the Landau damping term,  $\rho_{sc}$ , in the spectral function,

$$\int_0^\infty ds e^{-s/M^2} \frac{Im R^{phen.}(s)}{\pi} + \rho_{sc} = \left[ c_0 M^2 + c_1 + \frac{c_2'}{M^2} + \frac{c_3'}{2M^4} \right] \quad (41)$$

Where the primed symbols denote the corresponding in-medium quantities. The damping term originates due to the absorption of a space-like meson by an on-shell nucleon [30, 58].

The contributions for the vector and axial-vector meson channels are taken to be the same based on their scattering amplitudes with the nucleons [55, 58]. Incorporating the scattering term as,  $\rho_{sc} = \frac{\rho_B}{4M_N}$  [9, 55, 58, 59] in two channels (for both charged and neutral mesons with different  $c'_3$ ), the modified FESRs [Eqs.(35)-(37)], in medium are given by

$$F'_A = \left( c_0 s_0'^A + c_1 - f_\pi^2 - \frac{\rho_B}{4M_N} \right) \quad (42)$$

$$F'_A m_A'^2 = \left( \frac{c_0 (s_0'^A)^2}{2} - c_2' - f_\pi^2 m_\pi^2 \right) \quad (43)$$

$$F'_A m_A'^4 = \left( \frac{c_0 (s_0'^A)^3}{3} + c_3'^A - f_\pi^2 m_\pi^4 \right) \quad (44)$$

The in-medium FESRs for the vector meson channel [9] are thus modified to

$$F'_V = \left( c_0 s_0'^V + c_1 - \frac{\rho_B}{4M_N} \right) \quad (45)$$

$$F'_V m_V'^2 = \left( \frac{c_0 (s_0'^V)^2}{2} - c_2' \right) \quad (46)$$

$$F'_V m_V'^4 = \left( \frac{c_0 (s_0'^V)^3}{3} + c_3'^V \right) \quad (47)$$

The coefficient in the scalar four-quark condensate,  $\kappa_j$ , for the vector and axial-vector states, are determined by solving their respective vacuum FESRs. Once this factor is determined, the in-medium resonance parameters of the spectral function, i.e., mass,  $m'$ , the strength,  $F'$  and the threshold energy,  $s'_0$  can be obtained by solving the in-medium FESRs.

#### IV. IN-MEDIUM DECAY WIDTHS OF $A_1$ MESON

In this section, the hadronic decay modes of the light axial-vector meson,  $A_1$  going to a light vector meson,  $\rho$  and a pseudoscalar meson,  $\pi$  are investigated. It is an observed decay mode of the  $A_1$  meson, as given in the particle data group [60]. A phenomenological Lagrangian is introduced for the  $av\phi$  interaction (here,  $a, v, \phi$  denote the axial-vector, vector and pseudoscalar meson fields, respectively)

$$\mathcal{L}_{av\phi} = i\tilde{f}\langle a_{\mu\nu}[v^{\mu\nu}, \phi] \rangle. \quad (48)$$

Where, the  $SU(3)$  matrices of the mesons are considered as given in ref.[61]; The symbol  $\langle \rangle$ , denotes the trace of the product of matrices and  $i$  in front of  $\tilde{f}$  is to make the Lagrangian

hermitian. The spin-1 meson fields in Eq.(48) are treated as anti-symmetric tensor fields,  $a_{\mu\nu}$  and  $v_{\mu\nu}$  which transform under a non-linear realization of (local) chiral symmetry,  $G = SU(3)_L \times SU(3)_R$  as [62],

$$X_{\mu\nu} \xrightarrow{G} h(\phi')X_{\mu\nu}h(\phi')^\dagger, \quad X_{\mu\nu} = a_{\mu\nu}, v_{\mu\nu} \quad (49)$$

The chiral  $SU(3)_L \times SU(3)_R$  symmetry group is spontaneously broken down to  $SU(3)_V$  group. A non-linear realization of  $G$  [34], is defined on the elements  $u(\phi')$  of the coset space  $SU(3)_L \times SU(3)_R / SU(3)_V$  as

$$u(\phi') \xrightarrow{G} g_R u(\phi') h(\phi')^\dagger = h(\phi') u(\phi') g_L^\dagger; \quad g_{R,L} \in SU(3)_{R,L}, \quad h(\phi') \in SU(3)_V \quad (50)$$

where  $\phi'$  are the Goldstone boson fields and  $\phi = \frac{1}{\sqrt{2}} \sum_{i=1}^8 \lambda_i \phi'_i$ . The elements of the coset space are defined as,  $u(\phi') = \exp(-\frac{i}{\sqrt{2}} \frac{\phi}{f})$ . The vector, axial-vector and pseudoscalar meson fields transform as octets under  $SU(3)_V$ . If the  $SU(3)$  multiplets are denoted by  $S$  then, the non-linear realization of  $G$  leads to the following transformations

$$S \xrightarrow{G} h(\phi') S h(\phi')^\dagger, \quad S = a, v, \phi \quad (51)$$

The transformations, Eqs.(49)-(51) preserve the symmetry of the Lagrangian. Thus, a phenomenological Lagrangian has been used for the  $A_1 \rho \pi$  vertices (along with the other vertices in the octet of mesons), to find the decay widths of  $A_1 \rightarrow \rho \pi$  channels [61]. To calculate the hadronic decay widths for various ( $A_1 \rightarrow \rho \pi$ ) channels, the amplitudes are derived from the above Lagrangian. The various strong decay modes of axial-vector mesons going to vector and pseudoscalar mesons are noted in refs.[60]-[61]; among them most of the decays are only observed, no exact data are given for the corresponding decay widths. The possible decay channels of  $J^{PC} = 1^{++}$  and  $J^{PC} = 1^{+-}$  family of axial-vector mesons have been considered with their respective branching ratio, consistent with the particle data group information in the global fit of the coupling parameters (here only  $\tilde{f}$  is needed) (table.(IV) of [61]). These fittings are described in detail in that reference using both  $J^{PC} = 1^{+-}$  and  $J^{PC} = 1^{++}$  nonets of axial-vector mesons, namely the class of the  $B_1$  and  $A_1$  mesons. The values of the fitted parameter,  $\tilde{f}$ , will be used here to find the in-medium partial decay widths of the  $A_1$  meson within the nuclear medium in presence of a background magnetic field, including the magnetic catalysis effect on their masses. For tree level calculations, one can use the form,  $(\partial_\mu X_\nu - \partial_\nu X_\mu)$  instead of  $X_{\mu\nu}$  for  $X = a, v$ . Normalization of these fields are given by [62]

$$\langle 0 | X_{\mu\nu} | X; p, \epsilon \rangle = \frac{i}{m_X} [p_\mu \epsilon_\nu(X) - p_\nu \epsilon_\mu(X)]. \quad (52)$$

$m_X$  denotes the mass of the  $X$  meson. The expression for the  $A_1 \rightarrow \rho\pi$  decay width can be written as

$$\Gamma_{A_1 \rightarrow \rho\pi} = \frac{q}{8\pi m_{A_1}^2} |\overline{\mathcal{M}}|^2 \quad (53)$$

Where,  $q$  is the momentum of the final state particles in the rest frame of the axial-vector meson, given by

$$q(m_{A_1}, m_\rho, m_\pi) = \frac{1}{2m_{A_1}} \left( [m_{A_1}^2 - (m_\rho + m_\pi)^2] \times [m_{A_1}^2 - (m_\rho - m_\pi)^2] \right)^{1/2} \quad (54)$$

The interaction terms corresponding to the  $A_1\rho\pi$  vertices as given by Lagrangian (48), are

$$\mathcal{L}_{A_1\rho\pi} = \sqrt{2}i\tilde{f} \left[ A_1^0 (\rho^- \pi^+ - \rho^+ \pi^-) + A_1^+ (\rho^+ \pi^0 - \rho^0 \pi^+) + A_1^- (\rho^0 \pi^- - \rho^- \pi^0) \right] \quad (55)$$

These terms result from the parity and charge conjugation conservation of the Lagrangian density. The amplitude, obtained from the interaction vertices, becomes

$$\mathcal{M} = \frac{-2\lambda_{av\phi}}{m_{A_1} m_\rho} (p' \cdot p \quad \epsilon' \cdot \epsilon - \epsilon' \cdot p \quad \epsilon \cdot p') \quad (56)$$

with  $p'$ ,  $\epsilon'$  and  $p$ ,  $\epsilon$  are the four-momenta and polarization vectors of the  $A_1$  and  $\rho$  mesons respectively. Thus, using the tensor field formalisms, one finds the gauge invariant amplitude for the decay process. The coefficients,  $\lambda_{av\phi} = \sqrt{2}i\tilde{f}$  (with the appropriate sign). Therefore, the decay width is given by Eq.(53) by using Eqs.((54)-(56)) and the invariant relations between four-momenta,  $p^2 = m_\rho^2$ ,  $p'^2 = m_{A_1}^2$  and  $2p \cdot p' = (m_{A_1}^2 + m_\rho^2 - m_\pi^2)$ ,

$$\Gamma_{A_1 \rightarrow \rho\pi} = \frac{|\lambda_{av\phi}|^2}{2\pi m_{A_1}^2} q \left( 1 + \frac{2q^2}{3m_\rho^2} \right) \quad (57)$$

## V. RESULTS AND DISCUSSIONS

In the present work, the in-medium masses of the light vector mesons,  $\rho^{0,\pm}$ ,  $\omega$  and the light axial-vector mesons,  $A_1^{0,\pm}$  are investigated in the isospin asymmetric nuclear medium, in presence of an external, strong magnetic field. The contribution from the Dirac sea polarization in presence of magnetic field, are taken into account to study the in-medium masses. Masses are computed within the QCD sum rule approach, by using the medium modified light quark and scalar gluon condensates and the parameters of QCD Lagrangian (the current quark masses,  $m_u$ ,  $m_d$ , and the QCD running coupling constant,  $\alpha_s$ ). The medium modifications of the condensates are obtained from the medium modified scalar

fields,  $\sigma$ ,  $\zeta$ ,  $\delta$  and  $\chi$ , within the chiral  $SU(3)$  model [as given by Eqs.(8)-(10) and Eq.(12)]. In the chiral  $SU(3)_L \times SU(3)_R$  model, the meson fields are considered as classical fields under the mean field approximations, leaving the contributions of only the time-like component of the vector fields and the scalar fields. Under this approximation, the coupled equations of motion of the four scalar fields ( $\sigma$ ,  $\zeta$ ,  $\delta$  and  $\chi$ ) are solved by considering the effects of the baryon density,  $\rho_B$ , and isospin asymmetry parameter,  $\eta$  ( $= \frac{\rho_n - \rho_p}{2\rho_B}$ ), through the number ( $\rho_{p,n}$ ) and scalar densities ( $\rho_{p,n}^s$ ) of protons and neutrons in the nuclear medium. Furthermore, the energy levels of the charged nucleons, i.e., protons are modified by the magnetic field, give rise to Landau energy levels. There is another effect coming from the magnetic field due to the anomalous magnetic moments of the nucleons in both the Fermi and Dirac sea of nucleons. The contribution of an external magnetic field on the Dirac sea are obtained by computing the fermionic tadpole diagrams (or, the nucleons one-loop, self-energy functions) with the magnetized fermionic propagator of the Dirac sea of nucleons. There comes an additional term in the scalar densities of protons and neutrons due to this magnetized Dirac sea effect. Thus, the effects of magnetic field on the Fermi and Dirac sea of nucleons are realized on the scalar fields, or, indirectly on the chiral condensates (equations (8)-(12)) via the number and scalar densities of the nucleons within the chiral effective model.

The present investigation is restricted to the cold nuclear matter effects. The light quark condensates ( $\langle \bar{q}q \rangle$ ;  $q = u, d$ ) and the scalar gluon condensate ( $\langle \frac{\alpha_s}{\pi} G_{\mu\nu}^a G^{a\mu\nu} \rangle$ ), thus obtained, are used to calculate the in-medium masses and other spectral parameters of the light axial-vector and vector mesons, by solving their respective finite energy sum rules [Eqs.(42)-(47)]. The values of the current quark mass, and running coupling constant, to be used in the present study are,  $m_u = 4$  MeV,  $m_d = 7$  MeV and  $\alpha_s = 0.3551$  [9, 32]. The vacuum masses of the light mesons are taken to be,  $m_{A_1} = 1230$  MeV;  $m_\rho = 770$  MeV and  $m_\omega = 783$  MeV [60]. By using the vacuum masses, vacuum FESRs (Eqs.(35)-(37) for  $A_1$ , and Eqs.(38)-(40) for  $\rho$ ,  $\omega$ ), are solved to obtain the coefficients,  $\kappa_j$  of the scalar four-quark condensates. The values obtained are,  $\kappa_1 = -2.204$  (for  $A_1^0$ );  $\kappa_2 = -2.485$  (for  $A_1^\pm$ ); and  $\kappa_3 = -8.804$  (for  $\rho^\pm$ ),  $\kappa = 7.237$  and  $\kappa = 7.789$  for the  $\rho^0$  and  $\omega$  mesons respectively. In the QCD sum rule study of light vector mesons [9], the values of  $\kappa_j = 7.236, 7.788, -1.21$  were obtained for  $j = \rho^0, \omega, \phi$  mesons respectively, by solving their corresponding vacuum FESRs. For the axial-vector mesons, there is an extra pion pole contribution in the spectral density function,

in addition to the  $A_1$  meson pole. In our study, the pion decay constant,  $f_\pi = 93.3$  MeV and the pion mass,  $m_\pi = 139$  MeV [38] remain fixed. The vacuum values of the perturbative continuum threshold,  $s_0$  and the resonance strength,  $F$  (both in  $GeV^2$ ) are thus found to be 1.266 and 2.114 (for  $\rho$  state), 2.268 and 2.755 (for  $A_1$  state) and 1.3046 and 0.2419 (for  $\omega$  state), respectively. The value of the nuclear matter saturation density,  $\rho_0 = 0.15 \text{ fm}^{-3}$  is used in our study [38].

In Fig.1, the in-medium masses of the neutral [plots (a)-(b)], as well as the charged [plots (c)-(d)],  $\rho$  meson are shown with variation in the magnetic fields,  $|eB|/m_\pi^2$ , at zero density and at nuclear matter saturation density,  $\rho_0$ . The enhanced values of the chiral condensates in terms of the scalar fields within the chiral model, leads to the magnetic catalysis effect. Thus, incorporation of the magnetized Dirac sea polarization leads to this catalysis effect. This effects are studied on the masses apart from the Landau quantization of the magnetized Fermi sea of protons. The  $\rho$  mesons masses are seen to rise with magnetic field, accounting for the effects of magnetic catalysis, whereas there is almost no variation in absence of this effect. The different behavior can also be seen for isospin symmetric ( $\eta = 0$ ) and asymmetric ( $\eta = 0.5$ ) nuclear matter. The anomalous magnetic moments (AMM) of the protons and neutrons are considered in all over the calculations, and comparison are shown with the situation when this effect is not considered. Fig.2 shows the same kind of behavior for the mass of the  $\omega$  meson. Although the masses at  $\rho_B = 0$  and  $\rho_0$  become largely separated for the  $\rho$  meson as compared to the  $\omega$  meson. In Fig.3, similar plots are made for the neutral [plots (a)-(b)], and the charged [plots (c)-(d)] axial-vector meson,  $A_1$  as a function of  $|eB|$  (in units of  $m_\pi^2$ ). For the axial-vector meson, the in-medium masses at  $\rho_0$  are slightly larger as compared to the vacuum mass, which is opposite in nature with its chiral partner,  $\rho$  meson. Although masses of both the  $\rho$  and  $A_1$  mesons, increase with magnetic field, as a consequence of the magnetized Dirac sea effect.

In Fig.4, masses are plotted as a function of the baryon density,  $\rho_B$  (in units of  $\rho_0$ ), at  $|eB| = 0$ . Masses are shown in plot.(a) for the neutral states, at isospin symmetric ( $\eta = 0$ ) as well as the asymmetric ( $\eta = 0.5$ ) nuclear matter and plot.(b) for the charged particle states. In-medium masses of  $\rho$  meson decrease with increasing density, that of  $\omega$  meson decrease first, then rises sharply with density. The mass of the light axial-vector meson,  $A_1$ , which is the chiral partner of the light vector meson,  $\rho$ , increases very slightly with density.

The in-medium partial decay widths for the hadronic decay modes,  $A_1^0 \rightarrow \rho^\pm \pi^\mp$  [plot (a)],



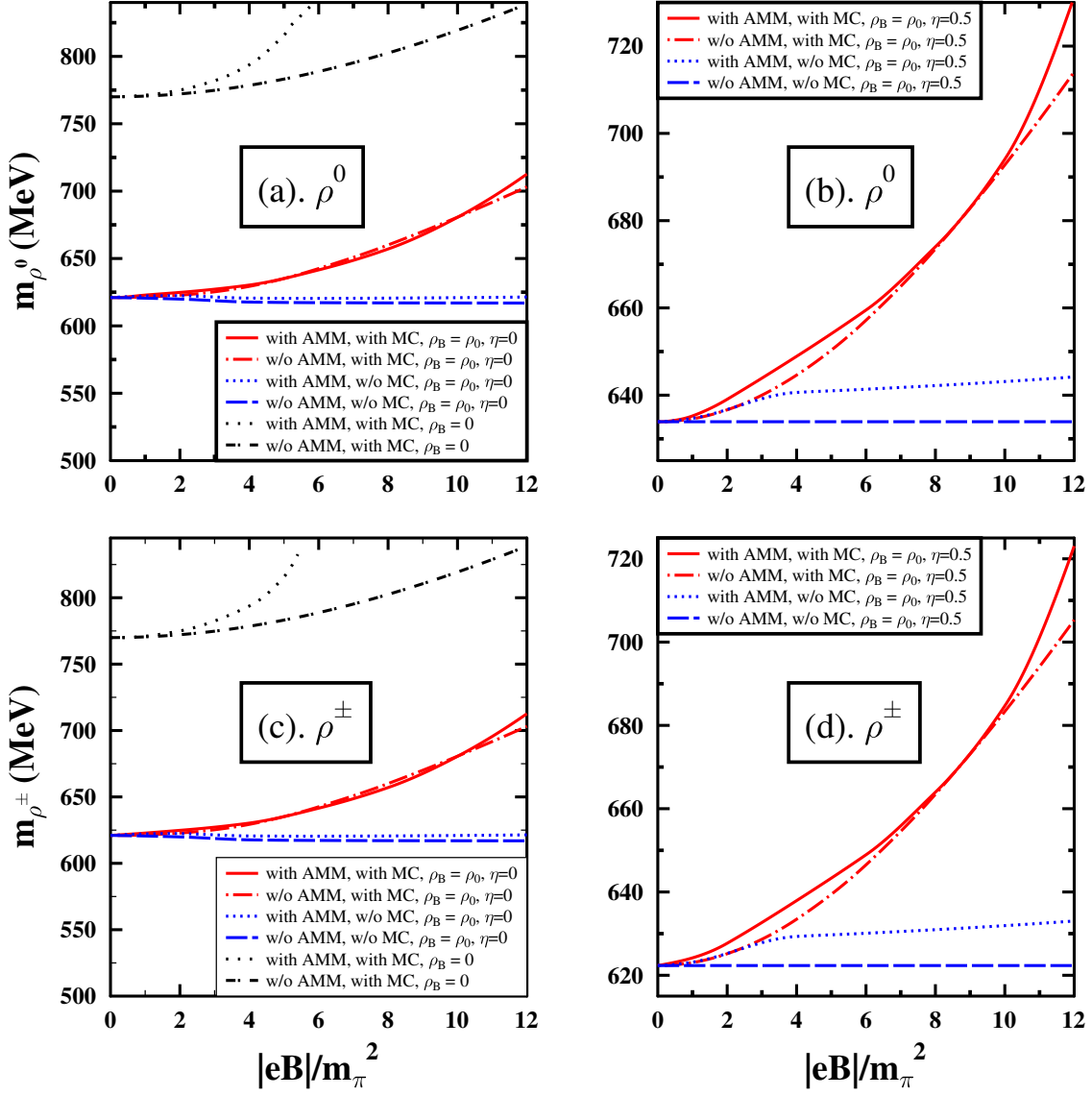


FIG. 1: In-medium masses of  $\rho^0$  [plots (a)-(b)] and  $\rho^\pm$  [plots (c)-(d)] states are plotted as a function of  $|eB|$  (in units of  $m_\pi^2$ ), at  $\rho_B = 0$ ,  $\rho_0$  and  $\eta = 0, 0.5$ . The magnetic catalysis (MC) effects on the masses, are compared with the case when there is no Dirac sea effect. Effects of nucleons anomalous magnetic moments (AMM) are considered and compared with the no AMM condition.

$A_1^\pm \rightarrow \rho^0 \pi^\pm$  [plot (b)] and  $A_1^\pm \rightarrow \rho^\pm \pi^0$  [plot (c)] are plotted in Fig.5, as a function of the magnetic field,  $|eB|/m_\pi^2$  at  $\rho_B = 0$ , accounting for the effects of Dirac sea polarization. The resulting catalysis effect on the masses, as calculated within the sum rule approach, lead to a lowering in the decay widths with increasing magnetic field for all three channels. By using the experimentally fitted values of the relevant decay modes as mentioned in

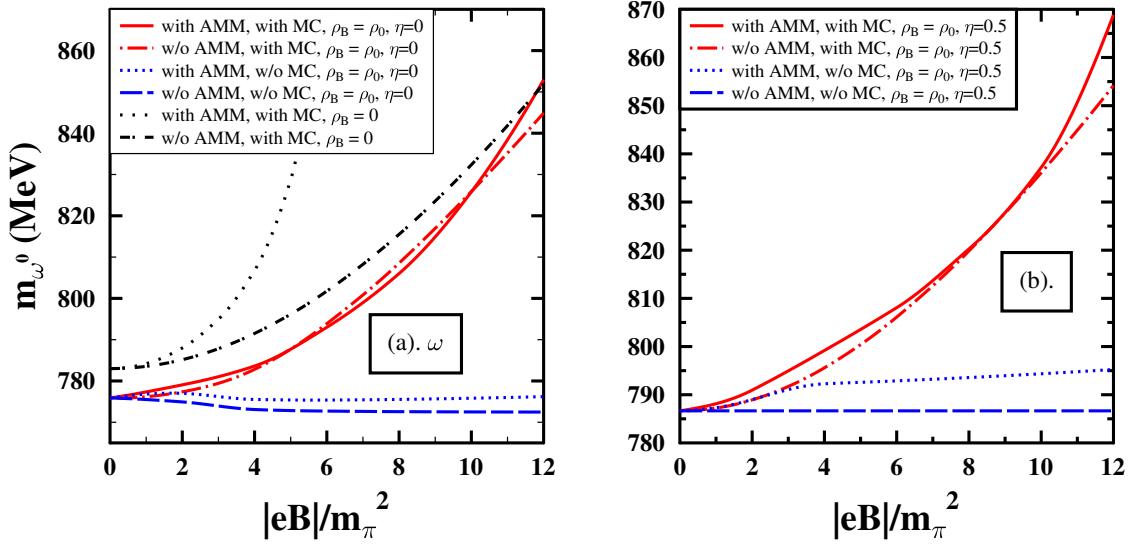


FIG. 2: In-medium masses of  $\omega$  [plots (a)-(b)] state are plotted as a function of  $|eB|$  (in units of  $m_\pi^2$ ), at  $\rho_B = 0$ ,  $\rho_0$  and  $\eta = 0$ ,  $0.5$ . The magnetic catalysis (MC) effects on the masses, are compared with the case when there is no Dirac sea effect. Effects of nucleons anomalous magnetic moments (AMM) are considered and compared with the no AMM condition.

table.(4) of Ref.[61], three set of values for the Lagrangian parameters were obtained. The values of  $\tilde{f} = 1270$  ( $f_1$ ), 1380 ( $f_2$ ) and 1540 ( $f_3$ ) in MeV, thus obtained are used in the present study to calculate the desired decay widths. The decay width for the  $A_1 \rightarrow \rho\pi$  mode, is calculated using Eq.(57), for all three parameters separately and the masses of the corresponding meson states as have already discussed before in this section. The mass of the neutral and charged pions to be used here are 135 MeV and 139.57 MeV respectively [60]. The vacuum decay widths for  $(A_1^0 \rightarrow \rho^\pm \pi^\mp)/(A_1^\pm \rightarrow \rho^0 \pi^\pm)/(A_1^\pm \rightarrow \rho^\pm \pi^0)$  channels are thus calculated to be 137.776/137.7756/138.3684 MeV, 162.6763/162.6758/163.3758 MeV and 202.5851/202.5845/203.4562 MeV, for  $\tilde{f} = f_1, f_2$  and  $f_3$  respectively. These values are very close to the central average value of 210 MeV (corresponding to the 50% branching ratio) for  $A_1 \rightarrow \rho\pi$  channel, as given in [61]. The phenomenological interaction Lagrangian contains no term involving  $A_1^0 \rho^0 \pi^0$  vertex, thus there is no decay for  $A_1^0 \rightarrow \rho^0 \pi^0$  mode. The authors of CLEO Collaboration [7] have been reported a branching ratio of about 60% for the intermediate  $\rho\pi$  ( $S$ -wave) state of  $A_1^-$  meson decaying into  $\pi^-\pi^0\pi^0$  relative to the total  $A_1^- \rightarrow \pi^-\pi^0\pi^0$  decay. The works of [63] have shown that,  $\rho\pi$  ( $S$ -wave) is the dominant decay channel for the ground state of  $A_1(1260)$  meson in the  $A_1$  family of axial-vector mesons

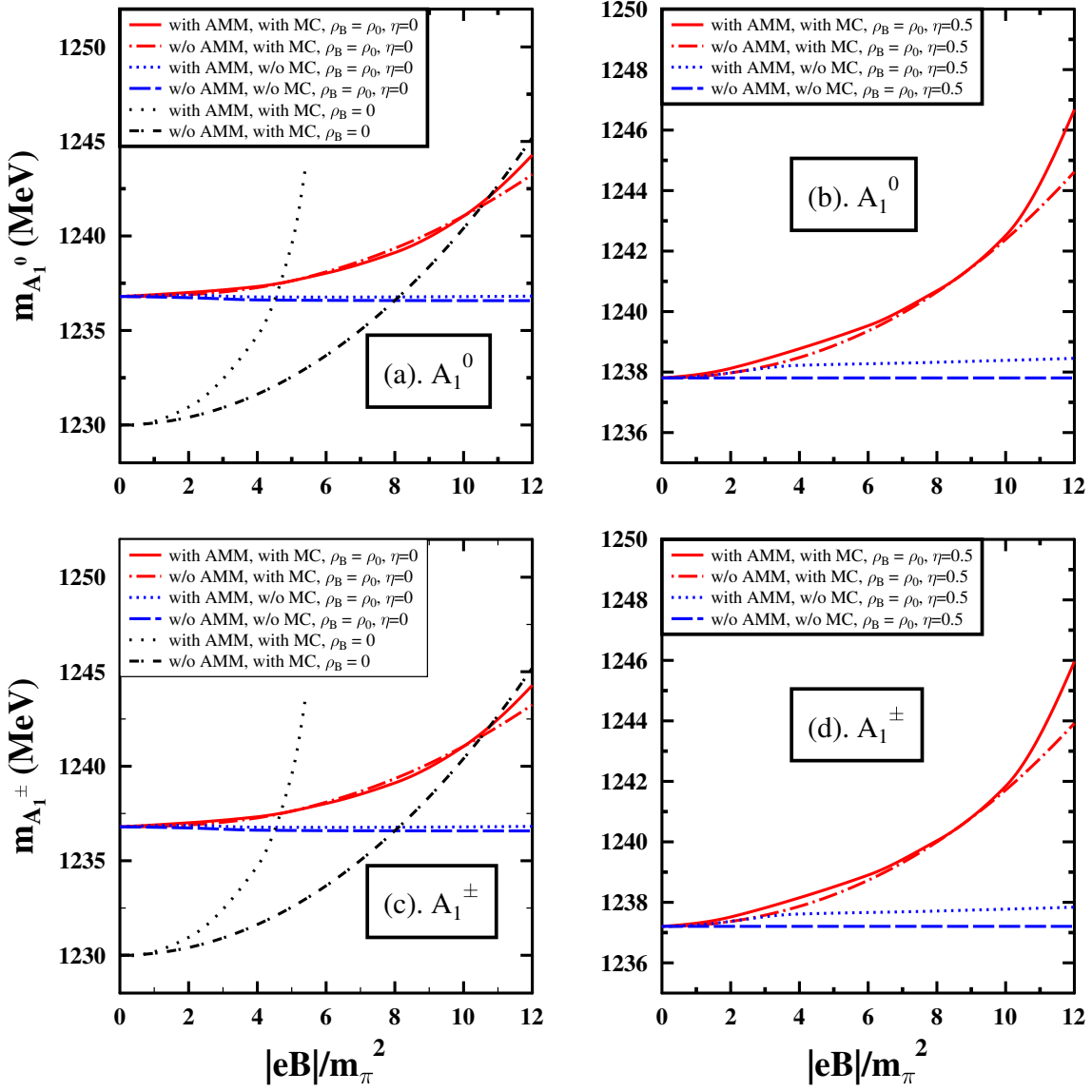


FIG. 3: In-medium masses of  $A_1^0$  [plots (a)-(b)] and  $A_1^\pm$  [plots (c)-(d)] states are plotted as a function of  $|eB|$  (in units of  $m_\pi^2$ ), at  $\rho_B = \rho_0$  and  $\eta = 0, 0.5$ . The magnetic catalysis (MC) effects on the masses, are compared with the case when there is no Dirac sea effect. Effects of nucleons anomalous magnetic moments (AMM) are considered and compared with the no AMM condition.

with quantum numbers ( $I^G(J^{PC}) = 1^-(1^{++})$ ). They have analyzed the mass spectra of all possible light axial-vector meson states by Regge trajectory analysis and have applied a quark pair creation model [64] to calculate the OZI-allowed strong decays of these mesons.

In Figs. [(6)-(8)], the in-medium partial decay widths for the three possible channels, ( $A_1^0 \rightarrow \rho^\pm \pi^\mp$ ), ( $A_1^\pm \rightarrow \rho^0 \pi^\pm$ ), ( $A_1^\pm \rightarrow \rho^\pm \pi^0$ ), respectively, are plotted as a function of

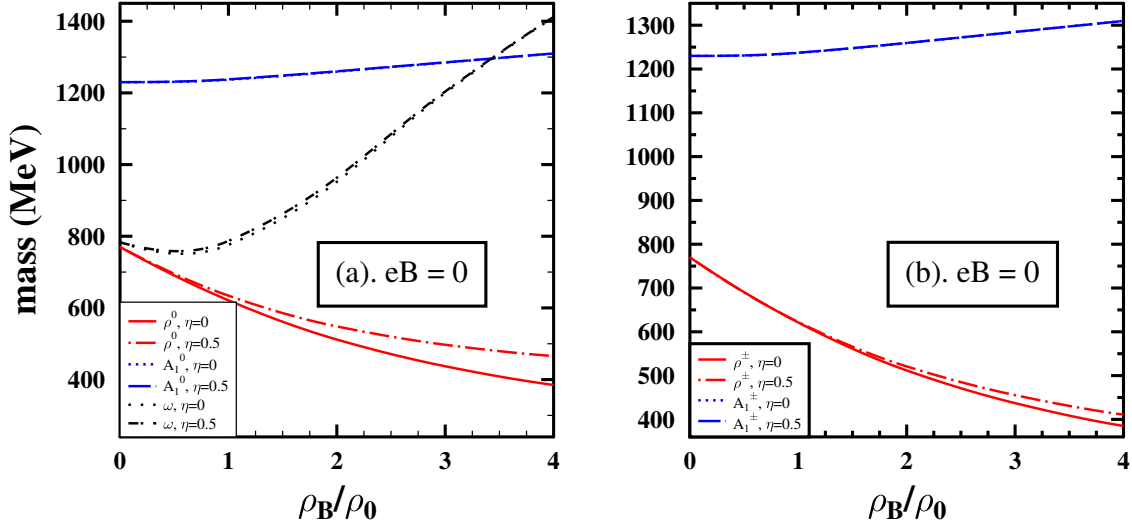


FIG. 4: The masses of the neutral mesons,  $\rho^0$ ,  $\omega$ ,  $A_1^0$  [plot (a)] and charged particle states  $\rho^\pm$ ,  $A_1^\pm$  [plot (b)] are plotted as a function of the relative baryon density,  $\rho_B/\rho_0$ , at zero magnetic field ( $|eB| = 0$ ) and for the isospin asymmetry parameter,  $\eta = 0, 0.5$ .

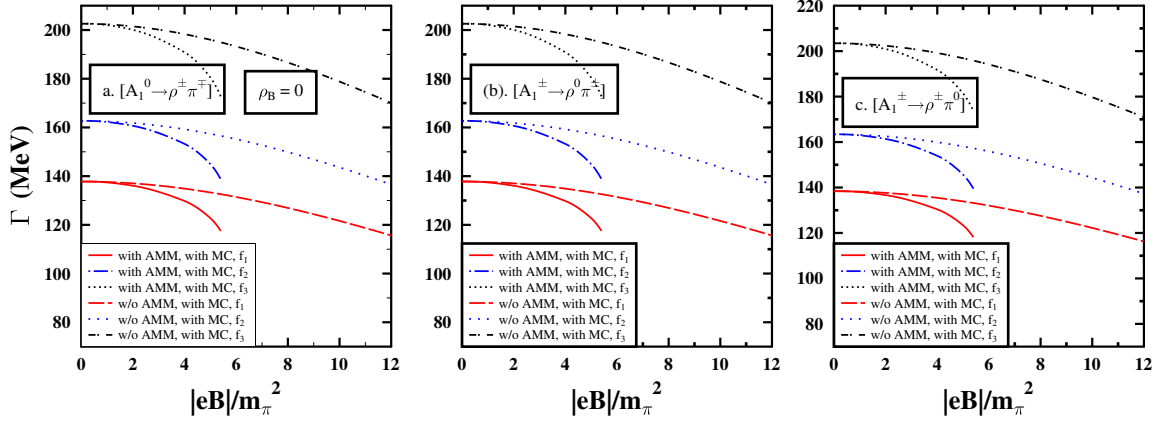


FIG. 5: The hadronic partial decay widths for the  $A_1^0 \rightarrow \rho^\pm \pi^\mp$  [plot (a)],  $A_1^\pm \rightarrow \rho^0 \pi^\pm$  [plot (b)] and  $A_1^\pm \rightarrow \rho^\pm \pi^0$  [plot (c)] channels, are plotted as a function of the magnetic field,  $|eB|/m_\pi^2$  at  $\rho_B = 0$ , accounting for the catalysis effects. Effects of nucleons anomalous magnetic moments (AMM) are compared with the case when AMM is not considered. The decay widths are shown for all three set of values of the coupling constant,  $f = f_1, f_2, f_3$ .

magnetic field, at  $\rho_B = \rho_0$  and  $\eta = 0, 0.5$ . The plots (a) and (c) in these figures show the effects of magnetic catalysis on the decay widths through their in-medium masses, both with

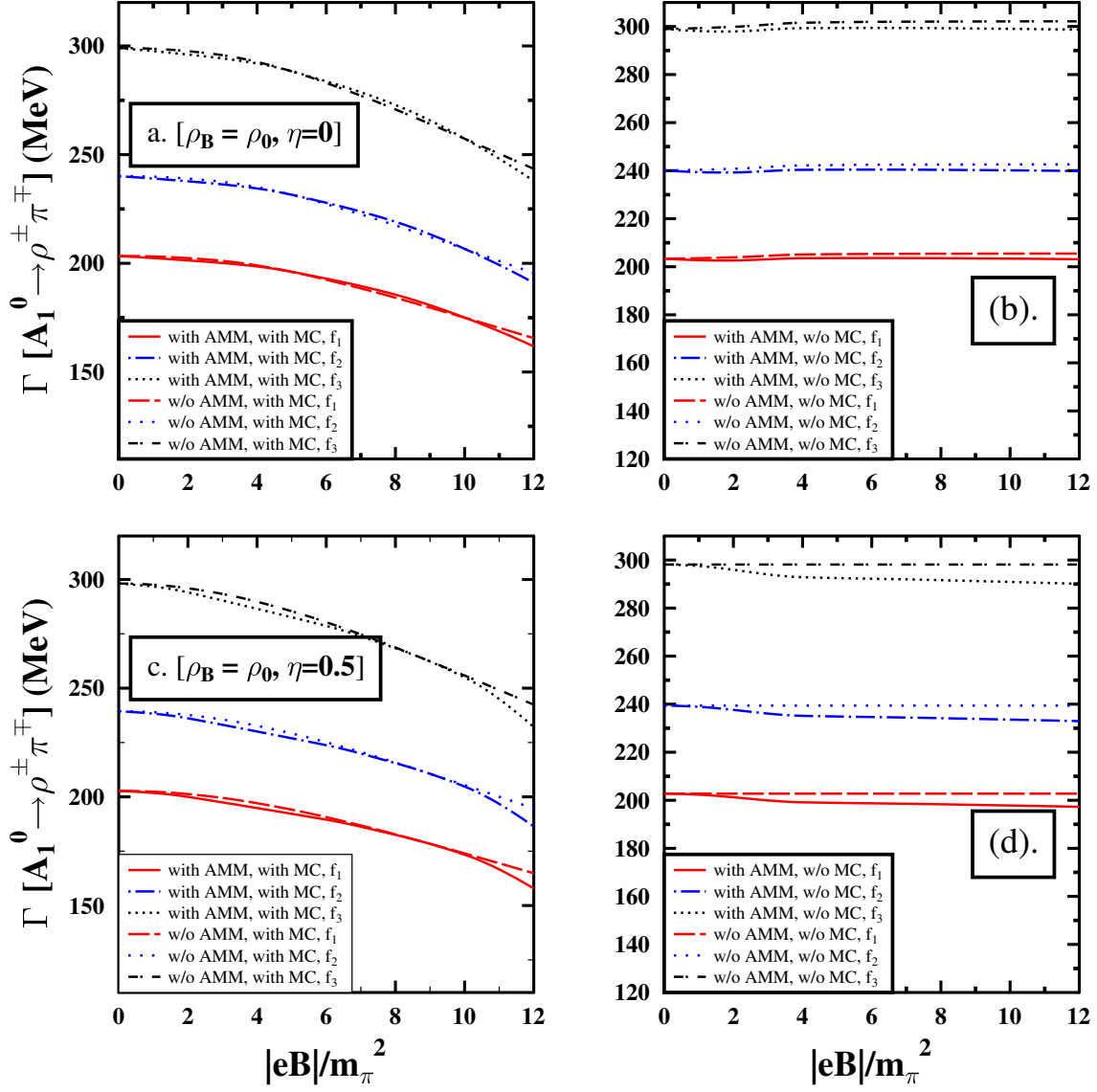


FIG. 6: The in-medium, partial decay widths for the  $A_1^0 \rightarrow \rho^\pm \pi^\mp$  mode, are plotted as a function of the magnetic field,  $|eB|/m_\pi^2$  at  $\rho_B = \rho_0$ , and for  $\eta = 0$  [plots (a)-(b)],  $\eta = 0.5$  [plots (c)-(d)]. The effects of magnetic catalysis (MC) [plots (a) and (c)] are compared with the case when there is no Dirac sea effect [plots (b) and (d)]. Comparison on the basis of nucleons anomalous magnetic moments are shown here. The decay widths are calculated and shown for three set of values of the coupling constant,  $f = f_1, f_2, f_3$ .

and without taking into account the anomalous magnetic moments of the nucleons. There is almost no changes in the decay widths with magnetic field, in the no sea approximation [plots (b) and (d)]. As the variation in masses are very small, without the effects of magnetic

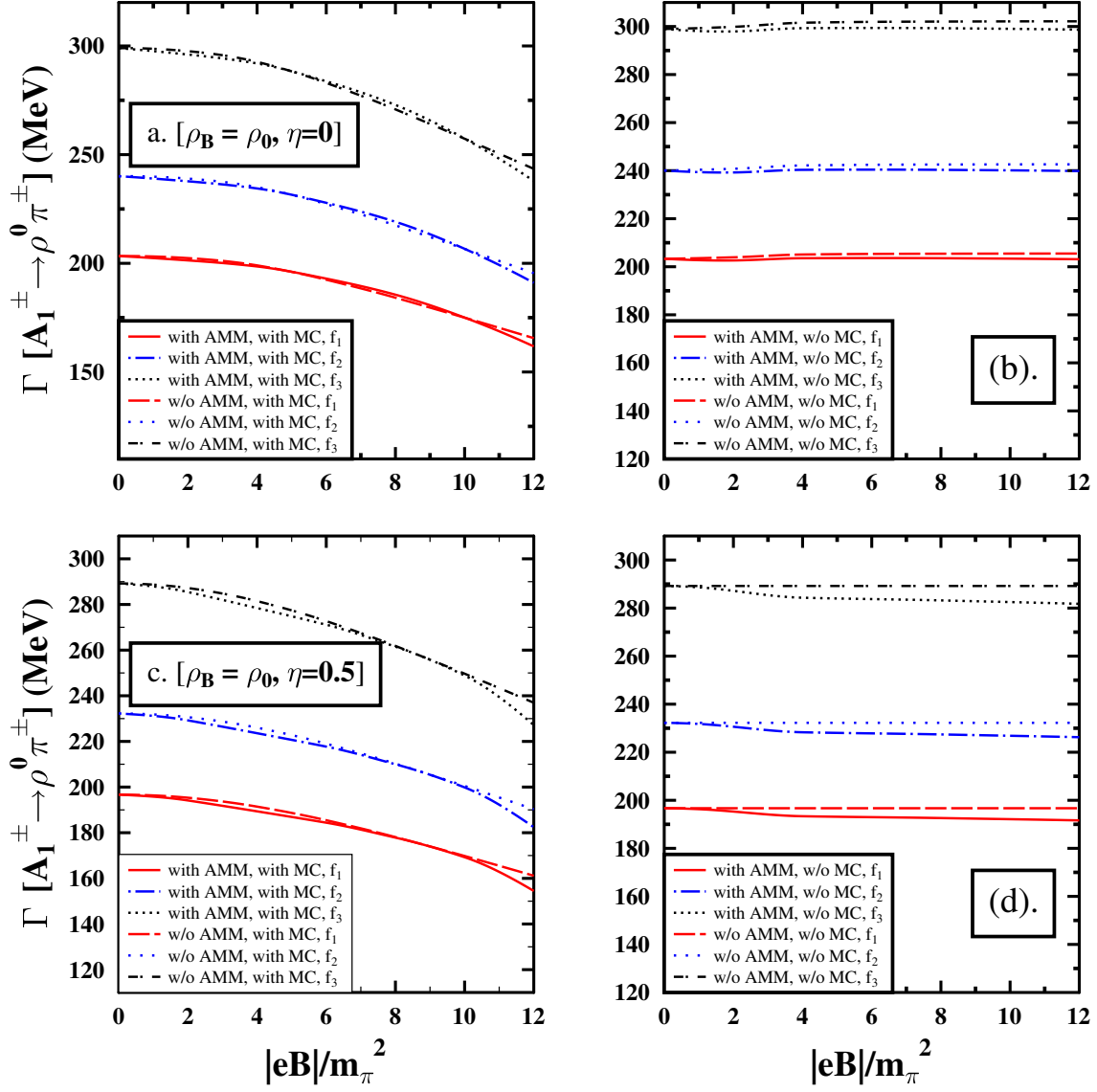


FIG. 7: The in-medium partial decay widths for the  $A_1^\pm \rightarrow \rho^0 \pi^\pm$  mode, are plotted as a function of the magnetic field,  $|eB|/m_\pi^2$  at  $\rho_B = \rho_0$ , and for  $\eta = 0$  [plots (a)-(b)],  $\eta = 0.5$  [plots (c)-(d)]. The effects of magnetic catalysis (MC) [plots (a) and (c)] are compared with the case when there is no Dirac sea effect [plots (b) and (d)]. Comparison on the basis of nucleons anomalous magnetic moments are shown here. The decay widths are calculated and shown for three set of values of the coupling constant,  $f = f_1, f_2, f_3$ .

catalysis. Finally, Fig.9 illustrates the variation of the in-medium decay widths as a function of  $\rho_B/\rho_0$ , in the absence of an external magnetic field ( $|eB| = 0$ ). Since the masses of the decay product,  $\rho$ , decrease as the density increases, with almost no changes in the parent

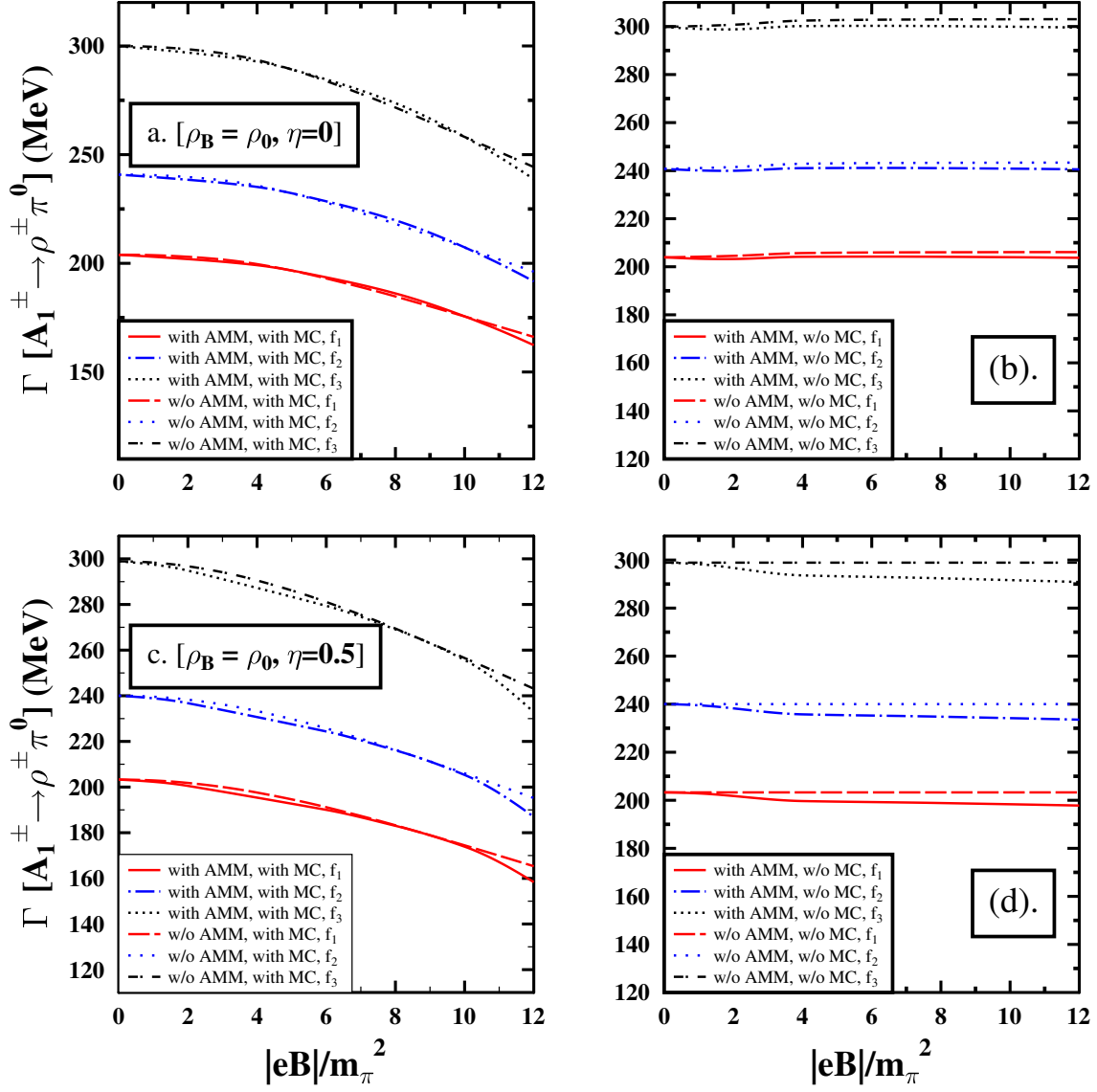


FIG. 8: The in-medium partial decay widths for the  $A_1^\pm \rightarrow \rho^\pm \pi^0$  mode, are plotted as a function of the magnetic field,  $|eB|/m_\pi^2$  at  $\rho_B = \rho_0$ , and for  $\eta = 0$  [plots (a)-(b)],  $\eta = 0.5$  [plots (c)-(d)]. The effects of magnetic catalysis (MC) [plots (a) and (c)] are compared with the case when there is no Dirac sea effect [plots (b) and (d)]. Comparison on the basis of nucleons anomalous magnetic moments are shown here. The decay widths are calculated and shown for three set of values of the coupling constant,  $f = f_1, f_2, f_3$ .

particle masses ( $A_1$  state), the decay widths are observed to rise with density. There is no in-medium effect considered on the pseudoscalar meson ( $\pi$ ) masses, in our present study.

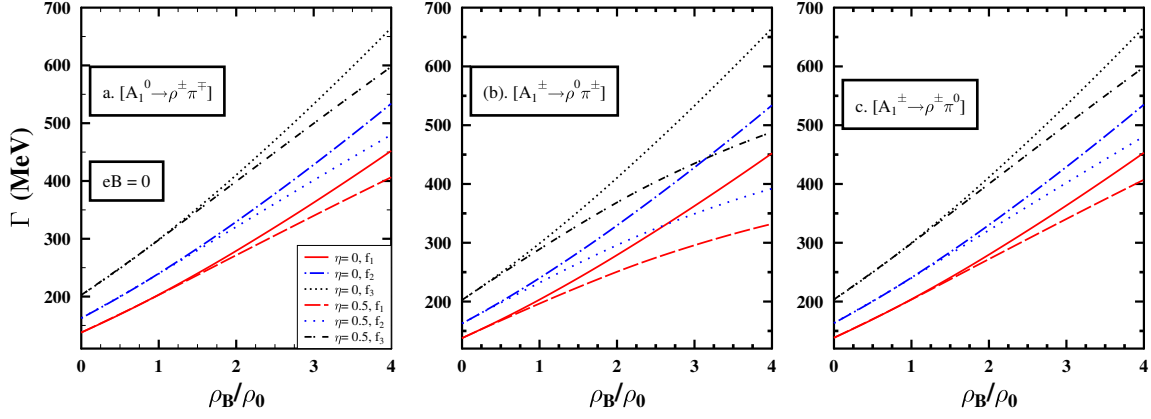


FIG. 9: The hadronic partial decay widths for the  $A_1^0 \rightarrow \rho^\pm \pi^\mp$  [plot (a)],  $A_1^\pm \rightarrow \rho^0 \pi^\pm$  [plot (b)] and  $A_1^\pm \rightarrow \rho^\pm \pi^0$  [plot (c)] modes of decay, are plotted as a function of the relative baryon density,  $\rho_B/\rho_0$ , at  $|eB|/m_\pi^2 = 0$ . The decay widths are shown for all three set of values of the coupling constant,  $f = f_1, f_2, f_3$ .

## VI. SUMMARY

In the summary, we have investigated the in-medium masses and hadronic decay widths of the light vector and axial-vector mesons in a magnetized nuclear matter, taking into account the effects of magnetic catalysis. The medium modifications of masses are calculated within the sum rule framework for the  $\rho^{0,\pm}$ ,  $\omega$  and  $A_1^{0,\pm}$  mesons, by applying the finite energy sum rules. Medium modifications of the other spectral parameters ( $F$ ,  $s_0$ ) can also be obtained. The in-medium masses are obtained in terms of the medium modified light quark (up to the scalar four-quark condensate) and the scalar gluon condensates. These condensates are calculated from the scalar fields, under the mean-field approximation, within the chiral  $SU(3)$  model. The contribution from an external magnetic field are studied on the masses and hence on the decay widths, by incorporating the field effects on the Fermi and Dirac sea of nucleons via the number and scalar densities of the protons and neutrons, on the scalar fields. The enhancement of the condensates with magnetic field, give rise to the catalysis effect, which lead to an increase in the masses of the light vector and axial-vector mesons. A phenomenological Lagrangian approach is adopted to account for the  $avp$  interaction vertices, in order to calculate the decay width of an axial-vector meson going to a vector



and a pseudoscalar meson, i.e.,  $A_1 \rightarrow \rho\pi$ . As the in-medium masses of the parent and daughter particles ( $A_1$  and  $\rho$ , respectively) increase with the field due to the catalysis effect, the corresponding partial decay widths for the possible modes of  $A_1 \rightarrow \rho\pi$  channel, decrease with rising magnetic field, accounting for the catalysis effect. There is almost no medium effects on the masses and decay widths, with the variation in magnetic field, when the catalysis effect is not considered. Thus, the appreciable changes in the in-medium properties of the  $\rho$ ,  $\omega$  and  $A_1$  mesons, due to the magnetic catalysis effect, at finite magnetic field, may affect the experimental observables in the peripheral, ultra relativistic, heavy-ion collision experiments, where produced magnetic field is huge.

- 
- [1] D. Kharzeev, L. McLerran and H. Warringa, Nucl. Phys. A **803**, 227 (2008).
  - [2] K. Fukushima, D. E. Kharzeev and H. J. Warringa, Phys. Rev. D **78**, 074033 (2008).
  - [3] V. Skokov, A. Y. Illarionov and V. Toneev, Int. J. Mod. Phys. A **24**, 5925 (2009).
  - [4] W. T. Deng and X.G.Huang, Phys.Rev. C **85**, 044907 (2012).
  - [5] K. Tuchin, Adv. High Energy Phys. **2013**, 490495 (2013).
  - [6] R. Rapp and J. Wambach, Adv. Nucl. Phys. **25**, 1 (2000).
  - [7] D. M. Asner et al. (CLEO Collaboration), Phys. Rev. D **61**, 012002 (1999).
  - [8] L.J. Reinders, S. Yazaki and H.R. Rubinstein, Nucl. Phys. B**196** (1982) 125-146.
  - [9] Amruta Mishra, Phys. Rev. C **91**, 035201 (2015).
  - [10] A. Bazavov, T. Bhattacharya, M. Cheng, et al., Phys. Rev. D **85** (2012) 054503.
  - [11] S. Borsanyi, et al., Wuppertal–Budapest Collaboration, JHEP 1009 (2010) 073.
  - [12] Igor Shovkovy, Lect. Notes Phys. **871**, 13 (2013); arXiv:1207.5081v2 [hep-ph] (2012).
  - [13] M. D’Elia, S. Mukherjee, and F. Sanfilippo, Phys. Rev. D **82**, 051501 (2010).
  - [14] D. Kharzeev, Ann. Phys. (N.Y.) **325**, 205 (2010); K. Fukushima, M. Ruggieri, and R. Gatto, Phys. Rev. D **81**, 114031 (2010).
  - [15] S.P. Klevansky, R.H. Lemmer, Phys. Rev. D **39**, 3478 (1989).
  - [16] V.P. Gusynin, V.A. Miransky, I.A. Shovkovy, Phys. Rev. D **52**, 4718 (1995).
  - [17] F. Preis, A. Rebhan, and A. Schmitt, Lect. Notes Phys. **871**, 51 (2013).
  - [18] D. P. Menezes, M. Benghi Pinto, S. S. Avancini, and C. Providencia, Phys. Rev. C **80**, 065805 (2009); D.P. Menezes, M. Benghi Pinto, S. S. Avancini, A. P. Martinez, and C. Providencia,

- Phys. Rev. C **79**, 035807 (2009).
- [19] Bhaswar Chatterjee, Hiranmaya Mishra, and Amruta Mishra, Phys. Rev. D **84**, 014016 (2011).
  - [20] Alexander Haber, Florian Preis, and Andreas Schmitt, Phys. Rev. D **90**, 125036 (2014).
  - [21] Arghya Mukherjee, Snigdha Ghosh, Mahatsab Mandal, Sourav Sarkar, and Pradip Roy, Phys. Rev. D **98**, 056024 (2018).
  - [22] G. S. Bali, F. Bruckmann, G. Endrodi, F. Gruber, and A. Schaefer, J. High Energy Phys. **04** (2013) 130.
  - [23] Paul M. Hohler and Ralf Rapp, Phys. Lett. B **731** (2014) 103–109.
  - [24] M.A. Shifman, A.I. Vainshtein and V.I. Zakharov, Nuclear Physics B **147** (1979) 448–518.
  - [25] L Govaerts, L. J. Reinders, F. De Viron and J. Weyers, Nucl. Phys. B **283** (1987) 706–722.
  - [26] Paul M. Hohler and Ralf Rapp, Nuclear Physics A **892** (2012) 58–72.
  - [27] S. Weinberg, Phys. Rev. Lett. **18** (1967) 507.
  - [28] J. I. Kapusta and E. V. Shuryak, Phys. Rev. D **49** 9 (1994).
  - [29] Tetsuo Hatsuda, Yuji Koike and Su Houn Lee, Nuclear Physics B **394** (1993) 221—264.
  - [30] Stefan Leupold, Phys. Rev. C **64**, 015202 (2001).
  - [31] Youngshin Kwon, Chihiro Sasaki, and Wolfram Weise, Phys. Rev. C **81**, 065203 (2010).
  - [32] Amruta Mishra, Ankit Kumar, Pallabi Parui, and Sourodeep De, Phys. Rev. C **100** 015207 (2019).
  - [33] S. Weinberg, Phys. Rev. **166** 1568 (1968).
  - [34] S. Coleman, J. Wess, B. Zumino, Phys. Rev. **177** 2239 (1969); C.G. Callan, S. Coleman, J. Wess, B. Zumino, Phys. Rev. **177** 2247 (1969).
  - [35] W. A. Bardeen and B. W. Lee, Phys. Rev. **177** 2389 (1969).
  - [36] A. Mishra, K. Balazs, D. Zschesche, S. Schramm, H. Stöcker, and W. Greiner, Phys. Rev. C **69**, 024903 (2004).
  - [37] D. Zschesche, A. Mishra, S. Schramm, H. Stöcker and W. Greiner, Phys. Rev. C **70**, 045202 (2004).
  - [38] P. Papazoglou, D. Zschesche, S. Schramm, J. Schaffner-Bielich, H. Stöcker, and W. Greiner, Phys. Rev. C **59**, 411 (1999).
  - [39] J. Schechter, Phys. Rev. D **21**, 3393 (1980).
  - [40] J. Ellis, Nucl. Phys. B **22**, 478 (1970); B. A. Campbell, J. Ellis, and K. A. Olive, *ibid.* **345**, 57 (1990).

- [41] Sushruth Reddy P., Amal Jahan C. S., Nikhil Dhale, Amruta Mishra and Jürgen Schaffner-Bielich, *Phys. Rev. C* **97** 065208 (2018).
- [42] Nikhil Dhale, Sushruth Reddy P, Amal Jahan CS, Amruta Mishra, *Phys. Rev. C* **98**, 015202 (2018).
- [43] Amal Jahan C.S., Nikhil Dhale, Sushruth Reddy P., Shivam Kesarwani, and Amruta Mishra, *Phys. Rev. C* **98**, 065202 (2018).
- [44] A. Broderick, M. Prakash, and J. M. Lattimer, *Astrophys. J.* **537**, 351 (2002).
- [45] A. E. Broderick, M. Prakash, and J. M. Lattimer, *Phys. Lett. B* **531**, 167 (2002).
- [46] F. X. Wei, G. J. Mao, C. M. Ko, L. S. Kisslinger, H. Stöcker, and W. Greiner, *J. Phys. G: Nucl. Part. Phys.* **32**, 47 (2006).
- [47] G. J. Mao, A. Iwamoto, and Z.-X. Li, *Chin. J. Astrophys.* **3**, 359 (2003).
- [48] Pallabi Parui, Sourodeep De, Ankit Kumar, and Amruta Mishra, arXiv:2208.05856v1 [hep-ph] (2022).
- [49] A. Mishra and A. Mazumdar, *Phys. Rev. C* **79**, 024908 (2009).
- [50] T. D. Cohen, R. J. Furnstahl, and D. K. Griegel, *Phys. Rev. C* **45**, 1881 (1992).
- [51] A. Kumar and A. Mishra, *Phys. Rev. C* **82**, 045207 (2010).
- [52] E. K. Heide, S. Rudaz, and P. J. Ellis, *Nucl. Phys. A* **571**, 713 (2001).
- [53] M. Urban, M. Buballa, J. Wambach, *Nucl. Phys. A* **697**, (2002) 338–371.
- [54] Taesoo Song, Tetsuo Hatsuda and Su Houng Lee, *Phys. Lett. B* **792** (2019) 160–169.
- [55] F. Klingl, N. Kaiser, and W. Weise, *Nucl. Phys. A* **624**, 527 (1997).
- [56] Philipp Gubler, Teiji Kunihiro and Su Houng Lee, *Phys. Lett. B* **767** (2017) 336–340.
- [57] S. Zschocke, O.P. Pavlenko, and B. Kämpfer, *Eur. Phys. J. A* **15**, 529–537 (2002).
- [58] W. Florkowski and W. Broniowski, *Nucl. Phys. A* **651**, 397 (1999).
- [59] T. Hatsuda, S. H. Lee, and H. Shiomi, *Phys. Rev. C* **52**, 3364 (1995).
- [60] P.A. Zyla et al. (Particle Data Group), *Prog. Theor. Exp. Phys.* **2020**, 083C01 (2020).
- [61] L. Roca, J. E. Palomar, and E. Oset, *Phys. Rev. D* **70**, 094006 (2004).
- [62] G. Ecker, J. Gasser, A. Pich, and E. de Rafael, *Nucl. Phys. B* **321**, 311 (1989).
- [63] Kan Chen, Cheng-Qun Pang, Xiang Liu and Takayuki Matsuki, *Phys. Rev. D* **91** 074025 (2015).
- [64] L. Micu, *Nucl. Phys. B* **10**, 521 (1969).